DISSIPATION SCALING IN WIND TURBINE WAKES EXPOSED TO FREESTREAM TURBULENCE

Oliver R. H. Buxton
Department of Aeronautics
Imperial College London, UK
o.buxton@imperial.ac.uk

Martin Bourhis
Department of Aeronautics
Imperial College London
m.bourhis@imperial.ac.uk

ABSTRACT

The nature of the dissipation of turbulent kinetic energy is experimentally measured in the wake of a 0.58 m diameter model wind turbine exposed to various "flavours" of freestream turbulence (FST), produced by an active turbulence-generating grid. The Taylor Reynolds number of the turbulence within the wake is high, ranging between $250 \lesssim Re_\lambda \lesssim 1000$. The dimensionless dissipation coefficient, C_ε, is observed to be a function of Re_G^m/Re_L^n, where Re_G is a global Reynolds number based on the turbine diameter and Re_L is a local turbulent Reynolds number based on the integral scale, in the outer part of the wind-turbine wake. This is where the intermittency of the turbulence is observed to be at its greatest. This scaling is characteristic of dissipation that is out of equilibrium with the inter-scale flux of turbulent kinetic energy in the energy cascade. Conversely, in the central portion of the wake there is no clear scaling of C_ε with Re_G^m/Re_L^n. With the lowest intensity FST C_ε is observed to be almost constant in the streamwise extent $1 < x/D < 20$, which may reflect either classical Kolmogorov-type (equilibrium) turbulence or balanced non-equilibrium turbulence.

INTRODUCTION

Wind turbines are typically clustered together into wind farms as developers seek to maximise the power output from limited lease areas whilst minimising costs associated with foundations, cabling, maintenance, and other infrastructure. This clustering means that the turbulent wakes generated by upstream turbines become the (unsteady) inflow to downstream machines, thereby affecting the overall efficiency of the wind farm. Since wakes are fluxes of reduced momentum (and hence also kinetic energy) then downstream turbines immersed in the wakes of upstream machines produce less power and are susceptible to accelerated accumulation of fatigue damage. Being able to accurately, but computationally inexpensively predict the spreading of wind-turbine wakes from the basis of the underpinning physics is therefore an important aspect of wind-farm design and optimisation.

Wind-turbine wakes are observed to evolve into a self-similar fashion downstream of the region immediately adjacent to the turbine. A Gaussian shape is typically used to represent the self-similar functional form of the wake's velocity deficit profile (e.g. Bastankhah & Porté-Agel, 2014). Previous studies on self-similar axisymmetric turbulent wakes have yielded predictions on the axial scaling of the maximum (centreline) mean velocity deficit, Δu_C, and the wake width r_w with downstream distance, x. Classically, this was predicted in Townsend (1976) (and later formalised in George (1989)) to be $\Delta u_C \sim x^{-2/3}$ and $r_w \sim x^{1/3}$ for high Reynolds number flows past solid, axisymmetric objects. This theory was developed by using a closure (the Taylor dissipation scaling) on the self-similar form of the dissipation rate within the wake

$$\varepsilon = C_\varepsilon \frac{K^{3/2}}{\mathscr{L}}. \tag{1}$$

This assumes that the rate of dissipation (ε) of turbulent kinetic energy (K) is in equilibrium with the inter-scale flux of the turbulent kinetic energy (TKE) within the inertial range of the cascade of TKE. Here $\mathscr{L}$ is the integral length scale of the turbulence, being indicative of the size of the largest (energy-containing) eddies within the flow, and C_ε is a constant. Henceforth, we refer to this as the *equilibrium* scaling law.

More recently, observations show that C_ε can in fact be a function of the ratio of two different Reynolds numbers, a global Reynolds number Re_G (defined by inlet conditions) and a local, turbulent Reynolds number Re_L (defined using local turbulent length and velocity scales) (Vassilicos, 2015) such that $C_\varepsilon \sim Re_G^m/Re_L^n \neq$ const. For a wind turbine, its diameter D is typically used to form Re_G, since the forcing at the global scale occurs across the entire rotor plane, and henceforth $Re_D \equiv Re_G$. This scaling for C_ε violates the classical Richardson-Kolmogorov (equilibrium) phenomenology for the cascade of TKE and is hence referred to as a *non-equilibrium* dissipation scaling. If self-similar analysis akin to that of George (1989) is conducted with the non-equilibrium dissipation scaling replacing $C_\varepsilon =$ const. then alternative scalings for Δu_C and r_w are obtained.

$$\Delta u_C \sim \left(\frac{x-x_0}{\theta}\right)^{\frac{-2}{3-n}} \left(\frac{l}{\theta}\right)^{\frac{-2n}{3-n}} Re_G^{\frac{2(n-m)}{3-n}} \tag{2}$$

$$r_w \sim \left(\frac{x - x_0}{\theta}\right)^{\frac{1}{3-n}} \left(\frac{l}{\theta}\right)^{\frac{n}{3-n}} Re_G^{\frac{m-n}{3-n}} \qquad (3)$$

where θ is the momentum thickness, l is the characteristic length of the wake-generating body, and x_0 is a virtual origin. In turbulent, axisymmetric wakes produced by solid objects it has been observed that for sufficiently high Reynolds numbers $m \approx n \approx 1$ (Nedić *et al.*, 2013; Dairay *et al.*, 2015; Vassilicos, 2015). These values lead to the scalings of $\Delta u_C \sim x^{-1}$ and $r_w \sim x^{1/2}$.

It is noteworthy that much of the previous work considering the dissipation scaling in wakes has done so from two perspectives; i) the wake-generator is a solid body, and ii) the wake expands out into a non-turbulent environment. This simplifies the problem since there is only one "flavour" of turbulence within such a flow — that produced within the wake itself arising from mean shear — and not an interaction between two adjacent, but fundamentally different streams of turbulence. Secondly, solid wake-generators do not produce a flow through the wake-generator due to porosity. Both of these scenarios are those encountered in a wind-turbine wake; the rotor plane itself is porous meaning that there is a flow crossing the rotor plane and since wind turbines are situated within the turbulent atmospheric boundary layer (ABL) their wakes are exposed to background turbulence whose history is completely different to that of the wake-turbulence.

An important feature of the non-equilibrium dissipation theory is that it accommodates different values for m and n to describe wake behaviour in different types of flows. Stein & Kaltenbach (2019) postulated that the often-observed linear growth of wind turbine wakes (in the near-wake region) could be explained in terms of the non-equilibrium scaling law when $m \approx n \approx 2$; resulting in the scaling laws of $\Delta u_C \sim x^{-2}$ and $r_w \sim x^1$. The goal of the present work is to try and identify the nature of the dissipation rate in a wind-turbine wake exposed to high-Reynolds-number, atmospheric-like turbulence. In particular we seek to identify whether the wake turbulence follows an equilibrium or non-equilibrium scaling and whether this varies in different regions of the flow. Long-term this ought to yield a physical, as opposed to *ad hoc.* basis for the modelling of the spreading of wind-turbine wakes which we have noted is a vital facet of wind-farm design/optimisation.

METHODOLOGY

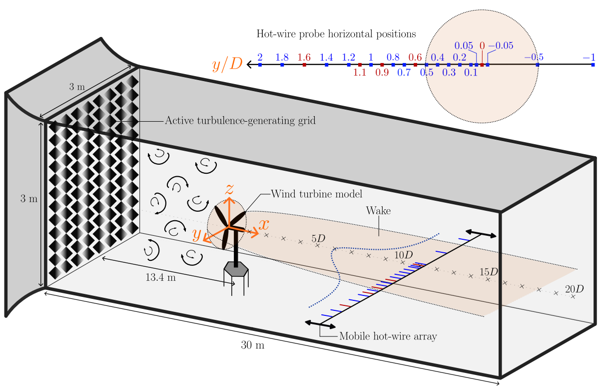

Figure 1: Experimental configuration highlighting the various hot-wire measurement stations

The experiments were performed in the 3 m $\times$ 3 m $\times$ 30 m test section of the large closed-loop wind tunnel at the University of Oldenburg using a wind turbine model with diameter $D = 0.58$ m. The Reynolds number based on D and freestream velocity U_∞ was $Re_D \approx 2.55 \times 10^5$. Since there was no pitch control on the blades, the turbine was operated at three different tip speed ratios, $\Gamma = \Omega D/(2U_\infty)$ where Ω is the turbine's rotational speed, in order to yield mild ($C_T \approx 0.5$), moderate ($C_T \approx 0.7$), and strong ($C_T \approx 0.9$) thrust coefficients to assess the influence of C_T on the dissipation scaling within the wake. Γ was controlled to be constant throughout the various tests. The outlet of the contraction nozzle is equipped with an active turbulence-generating grid, allowing for the generation of customised turbulent inflow conditions by using various grid-excitation protocols. Figure 1 shows the location of the turbine model with respect to the active grid, and the measurement stations (using single-component hot-wire sensors) in terms of the streamwise and cross-stream locations.

The active turbulence-generating grid was used to generate different "flavours" of freestream turbulence (FST). The objective was to explore the individual effects of the intensity of the FST, parameterised in terms of the turbulence intensity $TI = u'/U_\infty$, where u' is the r.m.s. velocity fluctuation measured at the location of the rotor plane of the turbine (in a preliminary experiment in which the turbine model is removed), and the length scale $\mathscr{L}$. In order to try to disentangle the individual effects of TI and $\mathscr{L}$ we selected grid protocols that generated FST flavours with i) a similar (small) $\mathscr{L}$ which are named SX, where X increases from 1 to 8 in order of increasing TI, ii) a similar (intermediate) TI with varying $\mathscr{L}$, denoted SX, MX, LX with S, M, and L denoting small, medium and large length scale, and iii) FST with a large $\mathscr{L}$ and varying TI denoted LX. These FST flavours are illustrated in figure 2.

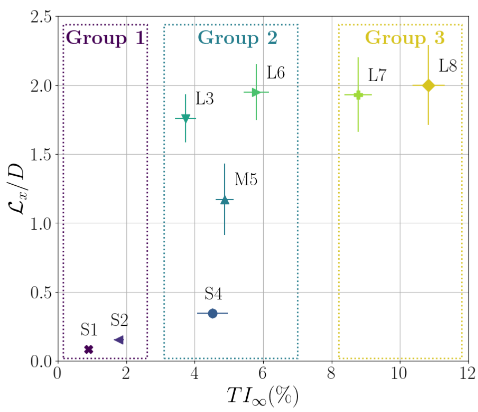

Figure 2: "Flavours" of FST generated by various grid-excitation protocols, parameterised in terms of intensity TI and length scale $\mathscr{L}$ of the FST.

The integral scale was computed by integrating the autocorrelation function (of time-lag τ) of the velocity fluctuations up to the first zero crossing, and subsequently using Taylor's frozen flow field hypothesis to convert a time scale into a length scale through the mean velocity U, i.e.

$$\mathscr{L} = U \int_0^{\tau_0} \rho_{uu}(\tau) \mathrm{d}\tau. \qquad (4)$$

Computation of C_ε requires an estimate of the dissipation rate $\varepsilon = 2\nu s_{ij}s_{ij}$, in which s_{ij} is the fluctuating rate-of-strain tensor. This in turn requires high spatial (and due to the way in which the dissipation rate is estimated, temporal) resolution. The sensing length for the hot-wire probes was 1.25 mm and the probes coloured in blue in figure 1 were sampled at 6 kHz whereas those coloured in red were sampled at 20 kHz. It is evidently not possible to measure the fully three-dimensional s_{ij} using single hot wire probes meaning that an assumption of local isotropy is required. The measurements were conducted sufficiently far downstream of the grid to justify this assumption (e.g. Mora *et al.*, 2019), although it was not assessed directly due to the measurement constraints. The dissipation rate was subsequently estimated by integrating the one-dimensional energy spectrum

$$\varepsilon = \int_0^{\kappa_{max}} 15\nu\kappa_1^2 E_{11}(\kappa_1)\mathrm{d}\kappa_1 \qquad (5)$$

where $E_{11}(\kappa_1) = E_{11}(f)U/2\pi$ is the one-dimensional power spectral density, $\kappa_1 = 2\pi f/U$ is the wavenumber with κ_{max} being the laregst resolved wavenumber, and f is the Fourier frequency. Note also that Taylor's frozen flow field hypothesis has again been used to convert from the frequency domain to the wavenumber domain. Taking the worst case scenario (highest turbulent Reynolds number) the sensing length of the hot-wire probes was $\ell \approx 3.4\eta$ and converting the sampling frequency into a spatial offset (using Taylor's hypothesis, i.e. $\delta x = U/f$) we recover a worst case scenario of $\delta x \approx 2.9\eta$. This suggests that our measurements, in the worst case scenario, are slightly under resolved which may result in a slight underestimate of the dissipation rate ε. The hot-wire probes sampled at 20 kHz, however, always ensured that $\kappa\eta = 2\pi f\eta/U \geq 1$ since it is the temporal velocity gradients, converted into spatial gradients through Taylor's hypothesis, that are most critical for dissipation rate estimates. Our spatio-temporal resolution is comparable to similar studies conducted in similar wind tunnels equipped with active turbulence-generating grids (e.g. Mora *et al.*, 2019).

Following Mora *et al.* (2019), the high-wavenumber dissipation range of the spectrum was fitted with a power law to eliminate the high-frequency noise contamination of the hot-wire data. It was estimated that the contribution to the overall dissipation estimate for the power-law fit to the high wavenumbers was below 7% of the estimated value of ε. The Taylor Reynolds number was subsequently computed as $Re_\lambda = \sqrt{\overline{u'^2}}\lambda/\nu$ with $\lambda = \sqrt{15\nu\overline{u'^2}/\varepsilon}$.

RESULTS AND DISCUSSION

Fields of C_ε for three illustrative FST flavours and $C_T \approx 0.5$ and $C_T \approx 0.9$ are presented in figure 3a and figure 3b, respectively. The flavours of FST are chosen such that the influence primarily of turbulence length scale can be deduced by comparing cases S1 and L3, and turbulence intensity can be deduced by comparing cases L3 and L8. It is observed that the dissipation coefficient is large in the vicinity of the shear layer produced in the tip region of the blades, but the coherence of this region of elevated C_ε is diminished as the intensity of the FST is increased. This corresponds to the well-known result that the presence of FST tends to erode the coherence of the tip-vortex system, with more intense FST intensity leading to a greater degree of erosion (e.g. Chamorro & Porté-Agel, 2009; Mikkelsen *et al.*, 2015). The figures also clearly show the discrepancy between the two adjacent streams of turbulence; that in the freestream (produced by the active turbulence-generating grid) and that in the wake (generated by the mean shear). An important observation is that C_ε in the freestream is typically larger than C_ε in the wake. A second important observation is that given that the two different streams of turbulence have different origins they will decay with different time scales; in fact given the mean shear within the wake it is not immediately clear that over the streamwise extent studied the turbulence is decaying.

The state of the turbulence within the wake can be characterised through the evolution of the turbulent (Taylor-based) Reynolds number, Re_λ, which is illustrated in figure 4. Figure 4a shows the evolution of Re_λ with streamwise distance, x, close to the wake centreline, $y/D \in [0, 0.05]$, whilst figure 4b shows $Re_\lambda(x)$ downstream of the blade-tip region, $y/D \in [0.4, 0.5]$. In both figures the results are presented for all flavours of FST illustrated in figure 2. The first observation is that the Taylor Reynolds number is high, exceeding $Re_\lambda = 200$ everywhere and attaining a maximum value of $Re_\lambda \approx 10^3$ in the near wake with the highest FST intensity. A very large difference can be observed for Re_λ when comparing against the FST flavour with the lowest and highest TI_∞; Re_λ can be observed to vary by as much as a factor of three. The primary difference between the data from the centreline and the tip-region is for $x/D \lesssim 5$, where the coherent motions associated to the tip-vortex system are observed to be the most energetic (Biswas & Buxton, 2024). At the farthest downstream measurement station, $x/D = 20$, there is little difference in Re_λ downstream of the centreline versus blade-tip region. We also observed that the Reynolds number stays relatively flat in the far wake, indicating that the turbulence is decaying only very slowly within the wake. Assessment of the equilibrium/non-equilibrium scaling of the dissipation rate naturally follows from this observation.

Figures 5a and 5b show the scatter plots of the dissipation coefficient C_ε for the various flavours of FST and measured at the various streamwise measurement locations plotted as a function of $\sqrt{Re_D}/Re_\lambda$ in order to illustrate the nature of the dissipation in the wind-turbine wake. Note that using the non-equilibrium scaling $\mathscr{L}/\lambda \sim Re_G^{1/2}$ from Mazellier & Vassilicos (2010) $\sqrt{Re_D}/Re_\lambda$ corresponds to Re_G^m/Re_L^n with $m = n = 1$. First, we consider the central portion of the wake. When $C_T \approx 0.5$ and $C_T \approx 0.7$, we observe relatively little scatter in the C_ε data for cases S1 to M5 (mild/intermediate intensity of the FST) and $C_\varepsilon \sim$ const. is as reasonable a fit as any to the data, which is indicative of either classical equilibrium dissipation or balanced non-equilibrium (Goto & Vassilicos, 2016). We also observe that the magnitudes of C_ε across the flavours of FST S1 to M5 is relatively insensitive to C_T (across all three thrust coefficients). However, when the wake turbulence intensity is amplified, by increasing C_T to ≈ 0.9, we observe a much greater degree of scatter on the C_ε data such that it is not reasonable to state $C_\varepsilon \sim$ const., but nevertheless there is no clear trend of C_ε with $\sqrt{Re_D}/Re_\lambda$. Perhaps, unsurprisingly, because these scenarios involve the interaction between two, relatively intense streams of turbulence that are adjacent to one another it is not possible to collapse the dissipation scaling, either in a classical equilibrium sense or in the non-equilibrium sense with a single turbulent Reynolds number. For the cases with the most intense FST, i.e. L8, there is a very large scatter of C_ε but this occurs at almost constant $\sqrt{Re_D}/Re_\lambda$ throughout the wake's evolution, commensurate with the Re_λ plateaus in figure 4. The dissipation coefficient can, in some sense, be thought of as the efficiency of the dissipation with respect to the cascade of TKE. This implies that for flavour L8, whilst the turbulence in the wake does not de-

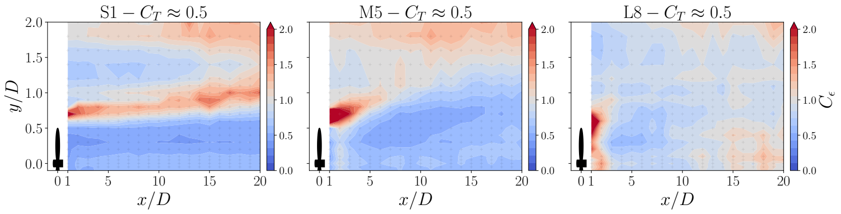

(a)

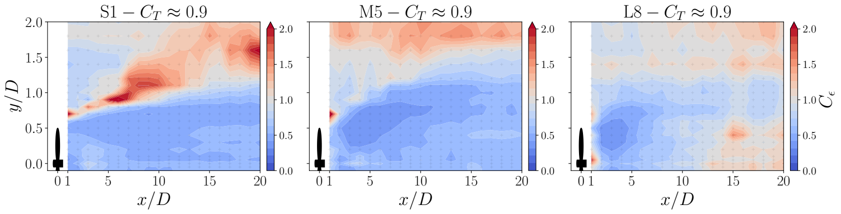

(b)

Figure 3: C_ε fields for three illustrative FST flavours at (a) $C_T \approx 0.5$ and (b) $C_T \approx 0.9$.

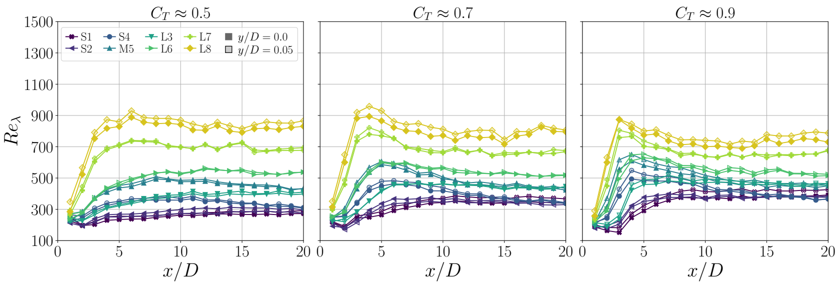

(a)

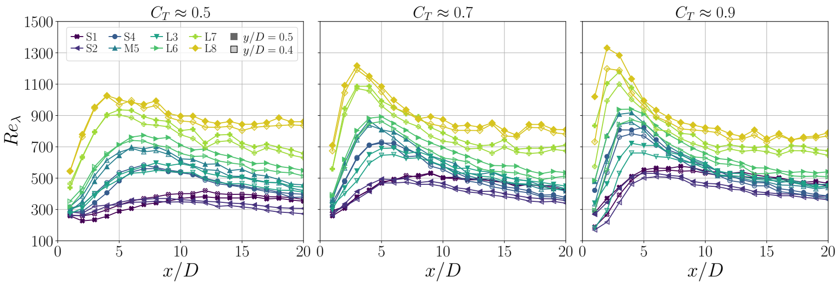

(b)

Figure 4: (a) Re_λ as a function of x close to the centreline of the wake for the various FST flavours illustrated in figure 2 and turbine thrust coefficients. (b) Re_λ as a function of x in the outer wake.

cay very much, $Re_\lambda(x) \approx$ const., the efficiency of the dissipation increases, presumably as a result of the mixing of the two streams of turbulence. This is illustrated in figure 3. As the thrust coefficient reduces from $C_T \approx 0.9$ to $C_T \approx 0.5$, and the ratio of the intensities of the wake turbulence to the FST reduces, C_ε increases. This result is suggestive of the fact that the interaction between two similar streams of turbulence somehow enhances the efficiency of the dissipation, reinforced by the observation that the smallest values for C_ε are observed for the smallest intensities of the FST.

The picture is, however, much clearer in the outer portion of the wake. For flavours of FST with mild/moderate TI_∞, and for all C_T values, there is a clear trend $C_\varepsilon \sim \sqrt{Re_D}/Re_\lambda$. This yields evidence that the dissipation follows a non-equilibrium dissipation scaling in the outermost portion of the wake. For the FST flavours with the highest TI_∞ there is a non-linear relationship between C_ε and $\sqrt{Re_D}/Re_\lambda$. The right-hand panel of the figure shows C_ε plotted as a function of Re_D/Re_λ^2 specifically for flavour L8 and $C_T \approx 0.5$, the scenario exhibiting the highest Re_λ in the far wake. The linear trend provides evidence that under a particular set of circumstances, perhaps relating to the similarity in intensities between the freestream turbulence and the wake turbulence, we exhibit a non-equilibrium dissipation scaling with $m \approx n \approx 2$; the non-equilibrium scenario that can explain a linear wake spreading rate.

Wind-turbine wakes are typically characterised as having a ring of enhanced intermittency surrounding the outermost part of the wake, a result first reported in Schottler *et al.* (2018). The intermittency is characterised in terms of the velocity increments extracted from the velocity time series, $\delta u(\tau) = u(t+\tau) - u(t)$, which can be computed over a range of time lags τ. τ can be converted into spatial increments using Taylor's frozen flow field hypothesis such that $\ell = \tau U(x,y)$, where U is the mean velocity, yielding velocity increments $\delta u(\ell)$. Probability density functions of δu for time lags corresponding to length scales D and $\mathscr{L}$ follow Gaus-

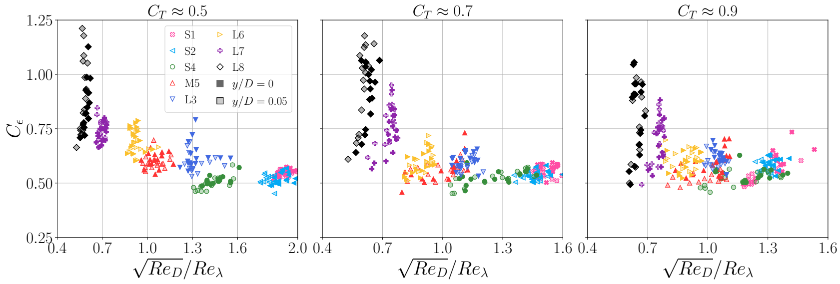

(a)

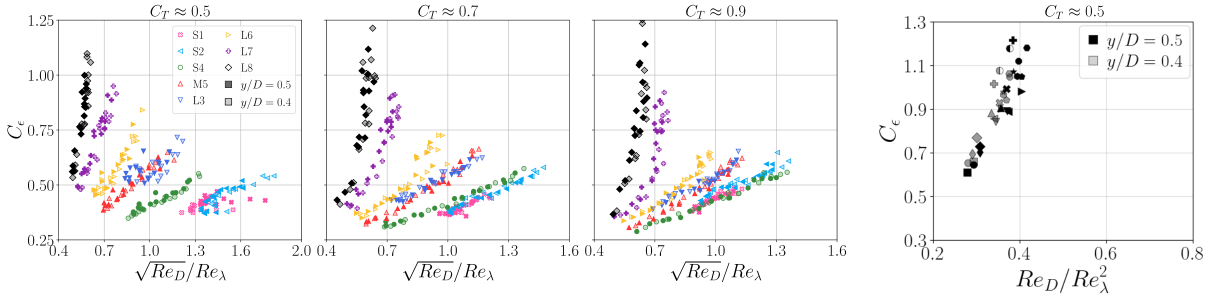

(b)

Figure 5: (a) C_ε as a function of x close to the centreline of the wake for the various FST flavours illustrated in figure 2 and turbine thrust coefficients. (b) C_ε as a function of x in the outer wake. In both cases data is extracted from $5 \leq x/D \leq 20$.

sian distributions, but increments at smaller length scales, i.e. $\ell = \lambda$ (the Taylor length scale in the freestream), are heavy tailed/intermittent.

Λ^2 is defined from the kurtosis of the velocity increments $F(\delta u)$, i.e.

$$\Lambda^2(\tau) = \frac{\ln[F(\delta u(\tau))/3]}{4} \tag{6}$$

$$F(\delta u(\tau)) = \frac{\overline{\delta u(\tau)^4}}{(\overline{\delta u(\tau)^2})^2}, \tag{7}$$

which is a metric that illustrates the intermittency of the velocity increments over time lag τ (distance ℓ). Figure 6 presents Λ^2 as a function of τ for two different turbine thrust coefficients and for the same FST flavours highlighted in figure 3. Focusing on case S1, we observe that regardless of the thrust coefficient, a band of elevated intermittency (high Λ^2) exists in the shear layer in the outermost part of the turbine wake. This intermittency persists all the way to the farthest downstream measurement station, at $x/D = 20$ and exists at both small time lags, and large time lags illustrating that intermittency co-exists at both small and large scales. The intermittency is enhanced at higher thrust coefficient. This is a perfect illustration of the type of intermittency ring discussed in previous work (e.g. Schottler *et al.*, 2018). This ring of intermittency coincides with the elevated C_ε illustrated in figure 3 and also the non-equilibrium dissipation scaling $C_\varepsilon \sim \sqrt{Re_D}/Re_\lambda$ illustrated in figure 5b. Contrastingly, we observe that in the central portion of the wake there is little to no intermittency and this coincides with the $C_\varepsilon \sim$ const. equilibrium dissipation scaling illustrated in figure 5a. We thus draw a link between the presence of intermittency and non-equilibrium dissipation scaling in wind-turbine wakes.

Case L8 shows a small enhancement of the intermittency, but only at small time lags. Whilst this enhanced intermittency is centred on the shear layer in the blade-tip region, it is far more diffuse than the intermittency ring observed for case S1 penetrating deeper into the wake. This intermittency is also observed to decay with streamwise distance, such that it only persists at small time lags in the far wake. Case L3 is in some sense intermediate between S1 and L8; whilst there is intermittency across all time lags it is particularly elevated at small τ, and whilst this intermittency is again focused in the outer portion of the wake it does tend to diffuse, and penetrate deeper into the wake with increased x. The intermittency is particularly enhanced for $C_T \approx 0.9$ in comparison to the lower thrust coefficient case. This corresponds to a much clearer scaling of $C_\varepsilon \sim \sqrt{Re_D}/Re_\lambda$ at $C_T \approx 0.9$ as opposed to $C_T \approx 0.5$. This again draws a link between intermittency and non-equilibrium dissipation. Contrastingly, for case L8 there is a strong variation of C_ε but it does not clearly exhibit a non-equilibrium dissipation scaling with $m \approx n \approx 1$ whilst concurrently exhibiting only a marginally enhanced intermittency at small scales. Crucially, this small-scale intermittency is diffuse within the flow reflecting the fact that two different streams of turbulence are interacting with one another in the outermost part of the wake that is exposed to intense FST. Given this interaction between two comparable streams of turbulence it is perhaps unsurprising that a scaling using a single turbulent Reynolds number is inadequate for capturing the nature of the cascade/dissipation. Comparing across all three flavours of FST, and both thrust coefficients we observe clear non-equilibrium dissipation scaling in the outermost portion of the wake only when intermittency is present at large scales (time lags); the presence of marginally elevated small-scale intermittency for case L8 yields variable C_ε, but no clear scaling.

CONCLUSIONS

Wind tunnel experiments were conducted using a 0.58 m diameter model wind turbine, operating at three different thrust coefficients and exposed to different "flavours" of freestream

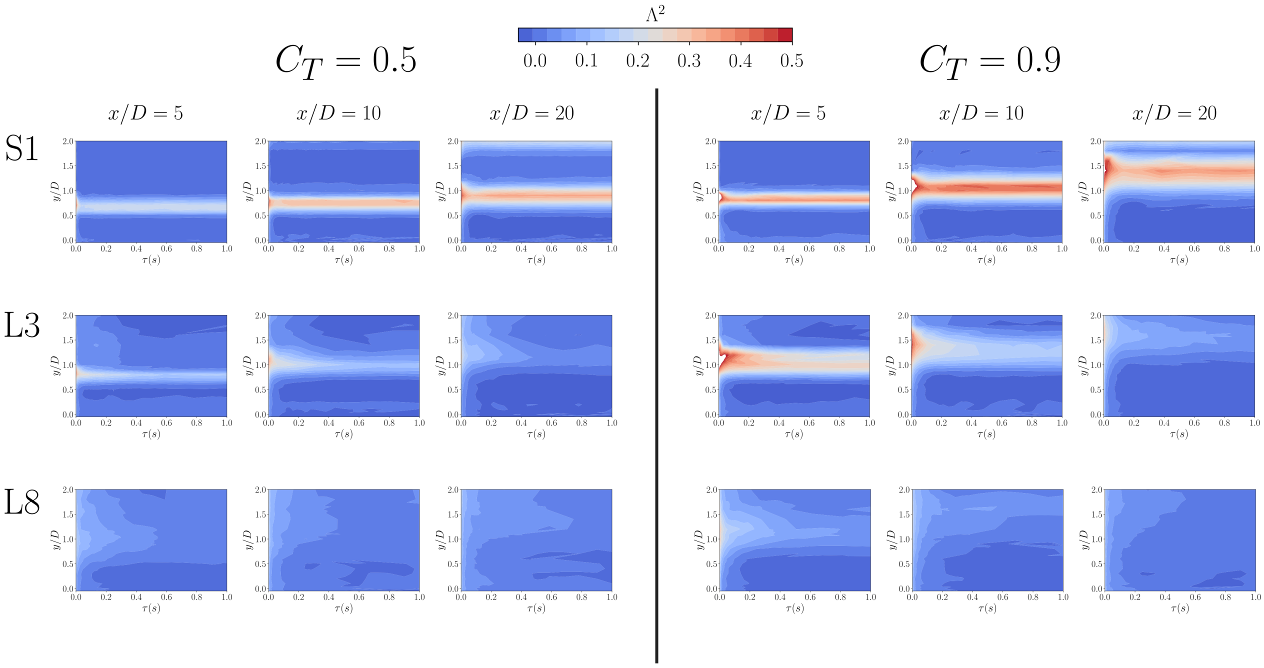

Figure 6: Intermittency parameter Λ^2 (see (6) plotted as a function of time lag τ for the various FST flavours of FST illustrated in figure 2 and two different turbine thrust coefficients.

turbulence (FST), produced by an active turbulence-generating grid. Measurements in the central portion of the wake revealed that for low intensity background turbulence the dissipation coefficient C_ε remained roughly constant, a result that is indicative of either classical equilibrium scaling of the dissipation rate or balanced non-equilibrium (Goto & Vassilicos, 2016). However, in the outer region of the wake there was a clear scaling $C_\varepsilon \sim \sqrt{Re_D}/Re_\lambda$ which is indicative of a particular type of non-equilibrium dissipation scaling corresponding to $C_\varepsilon \sim Re_G^m/Re_L^n$ with $m = n = 1$ for mild/moderate intensities of FST. This result is linked to the enhanced large-scale intermittency that is found in the outer portion of a wind-turbine wake, the so-called ring of intermittency. For more intense FST, in which there is less distinction between the wake-turbulence and the FST, some evidence is presented that in certain circumstances non-equilibrium dissipation can exist within the outermost portion of the wake with $m = n = 2$. In these circumstances, the intermittency is only elevated at small scales. At the highest intensities of FST, and particularly at the highest turbine thrust coefficient, a strong variation was observed in C_ε in the central portion of the wake but not one that can be described by the non-equilibrium dissipation scaling. It is presumed that this arises due to the interaction and mixing between two streams of turbulence meaning that a single turbulent Reynolds number is insufficient to fully capture the cascade/dissipation processes.

REFERENCES

Bastankhah, M. & Porté-Agel, F. 2014 A new analytical model for wind-turbine wakes. *Renewable Energy* **70**, 116–123.

Biswas, N. & Buxton, O.R.H. 2024 Effect of tip speed ratio on coherent dynamics in the near wake of a model wind turbine. *Journal of Fluid Mechanics* **979**, A34.

Chamorro, Leonardo P & Porté-Agel, Fernando 2009 A wind-tunnel investigation of wind-turbine wakes: boundary-layer turbulence effects. *Boundary-layer Meteorology* **132** (1), 129–149.

Dairay, T., Obligado, M. & Vassilicos, J.C. 2015 Non-equilibrium scaling laws in axisymmetric turbulent wakes. *Journal of Fluid Mechanics* **781**, 166–196.

George, W.K. 1989 The self-preservation of turbulent flows and its relation to the initial conditions and coherent structures. In *Advances in Turbulence*, pp. 39–73.

Goto, S. & Vassilicos, J. C. 2016 Unsteady turbulence cascades. *Physical Review E* **94**, 053108.

Mazellier, N. & Vassilicos, J.C. 2010 Turbulence without Richardson–Kolmogorov cascade. *Physics of Fluids* **22** (7).

Mikkelsen, Robert F, Henningson, Dan S, Ivanell, Stefan, Sarmast, Sasan, Andersen, S *et al.* 2015 Simulation of wind turbine wakes using the actuator line technique. *Philosophical Transactions of the Royal Society A: Mathematical, Physical and Engineering Sciences* **373** (2035).

Mora, D O, Muñiz Pladellorens, E, Riera Turró, P, Lagauzere, Muriel & Obligado, Martin 2019 Energy cascades in active-grid-generated turbulent flows. *Physical Review Fluids* **4** (10), 104601.

Nedić, J., Vassilicos, J.C. & Ganapathisubramani, B. 2013 Axisymmetric turbulent wakes with new nonequilibrium similarity scalings. *Physical Review Letters* **111** (14).

Schottler, J., Bartl, J., Mühle, F., Sætran, L., Peinke, J. & Hölling, M. 2018 Wind tunnel experiments on wind turbine wakes in yaw: redefining the wake width. *Wind Energy Science* **3** (1), 257–273.

Stein, V.P. & Kaltenbach, H.J. 2019 Non-equilibrium scaling applied to the wake evolution of a model scale wind turbine. *Energies* **12** (14), 2763.

Townsend, A.A.R. 1976 *The Structure of Turbulent Shear Flow*. Cambridge University Press.

Vassilicos, J.C. 2015 Dissipation in turbulent flows. *Annual Review of Fluid Mechanics* **46**, 95–114.